MMA Memo. 234

Thermal Behavior of the Leighton 10-m Antenna Backing Structure

James W Lamb and David P Woody
Owens Valley Radio Observatory
California Institute of Technology
23 October, 1998

Abstract: One of the OVRO antennas has been instrumented with 48 thermistors on the backing structure, and the data taken over a period of more than a month with a 2 min time resolution have been analyzed. The nighttime temperature is uniform within ~2 C while temperature differences across the structure of up to 12 C are observed during the day. There is a strong inverse correlation between wind speed and temperature variance and a weaker one on the direction of the sun and wind relative to the antenna pointing direction. Structural modeling shows that pointing and focus are strongly affected, but the effect on surface rms is at the level of 10 μm. By using the temperature information to correct the pointing and focus in real time it should be possible to effect a significant improvement in performance of the antennas.

1. Introduction

The Leighton 10-m antennas (Leighton [1]) at the Owens Valley Radio Observatory are steel structures with aluminum honeycomb sandwich panels. The performance is dominated during the daytime by thermal effects on the mount, the backing structure (BS), the secondary mirror supports, and the panels. These induce pointing and focus errors, as well as degrading the effective surface figure. An understanding of these effects is essential if we are to be able to reduce or correct for them. The information will also be the basis for evaluating designs for the MMA antennas.

The temperature distribution in the antenna is a function of the materials and optical and infrared emissivities of the surfaces. It is also determined by solar illumination, wind and the ambient temperature variations. Because of the many variables and the difficulties of evaluating heat transfer by conduction, forced and natural convection, etc., it is difficult to make an accurate model of the temperature distribution in the structure. For that reason, temperature measurements are necessary to achieve an accurate prediction of thermal performance. As a first step, the backing structure of one of the 10-m antennas has been outfitted with a set of 48 temperature sensors which are monitored during normal operation of the array.

Once the temperature distribution is known the structural changes can be evaluated. Analytical expressions derived which relate the effect of deformations of the primary reflector to gradients in the backing structure [2] give an idea of the magnitudes of deformation resulting from a given temperature profile, but more accurate evaluation requires finite element analysis. The structural changes can then be translated directly into pointing, focus, and surface error results.

The current set of data relates only to the BS. For a complete analysis the mount and secondary mirror supports should be included — these will be part of a later study. Panels will also be considered separately.

2. Instrumentation

The temperature sensors were YSI 44007 thermistors [3] in a monitoring scheme similar to that used by Lamb and Foster [4]. A voltage reference is applied to a resistor in series with the thermistor and the voltage across the resistor is measured using a data acquisition board in a PC. LabVIEW [5] is used to read the data and convert to temperature. With the choice of circuit components and cabling the matching of temperature readings is dominated by variations in

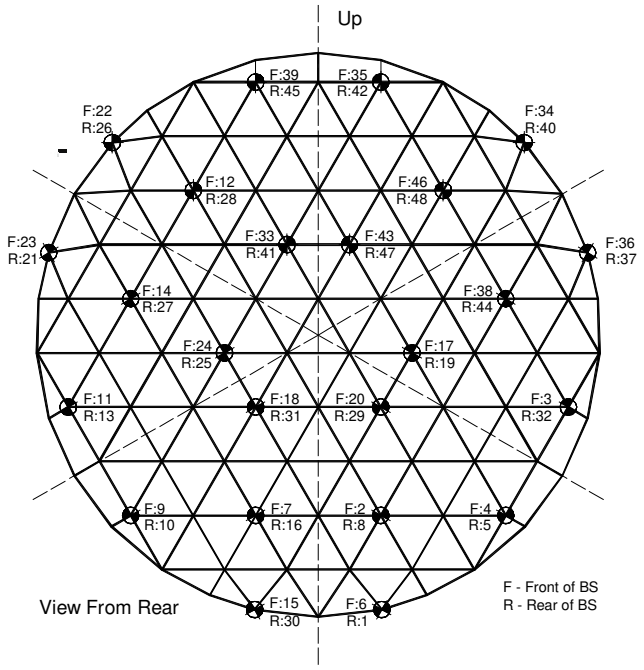

Figure 1: Positions of thermistors on backing structure.

thermistors which nominally have a ±0.2 C interchangeability. To verify this, the thermistors were mounted on an aluminum plate which was insulated to keep the sensors at a uniform temperature. The plate was slowly cycled over a range of about 20 C and the temperature readings compared. The rms variation was about 0.07 C and the maximum 0.2 C. By applying individual correction factors to each of the thermistor resistances the variability was reduced to an rms of about 0.035 C, more than adequate for the accurate characterization of the BS.

The thermistors were mounted in aluminum blocks with thermal conductivity epoxy (Stycast 2850 FT [6]) and the blocks then glued to the BS in the locations shown in Fig. 1. The acquisition PC was installed in the antenna sidecab and connected to the site Ethernet. Each measurement comprised 1000 samples that were averaged to reduce noise and obtain resolution of better than 1 bit on the 12-bit converter. Data were written to disk, typically at 2 min intervals, with a file for each day.

Weather information was taken from the standard OVRO weather database so that temperature distributions could be related to the wind and ambient temperature conditions. This information was obtained at the control building, about 200 m from the antenna. Antenna azimuth and elevation were also recorded simultaneously to be correlated with the sun and wind directions.

3. Measurements

A set of data covering over a month has been obtained for late April to early June 1998 under quite varied conditions, including clear and calm, clear and windy, and overcast. Under overcast conditions the variation in temperature across the antenna is small, similar to the nighttime case. Some of the plots show that when cloud cover comes in, the antennas can become isothermal within 10 to 15 min. In the subsequent discussions only data from clear days will be considered since these correspond to the best observing conditions. They are also more representative of the 5 000 m site for the MMA.

A typical set of data is shown in Fig. 2. At night the structure is quite isothermal, while significant gradients develop during the day with differences of up to 8 C being observed in this case. Differences up to 12 C were observed on other days. Usually the greatest variance is seen near sunrise when solar heating starts but the wind is low. Clearly there are other systematic patterns in the distribution of temperatures on shorter time scales.

At any given time the temperature distribution may be decomposed into gradients between the front and rear, and vertical, horizontal, and radial gradients. The horizontal and vertical gradients affect primarily the pointing, and the radial and front to rear differences alter the focus. Rates of change of temperature can be as high as 1.5 C min^{-1} at any given sensor so that the structure responds quickly to changing environmental conditions. Fig. 2(*a*) also shows the ambient temperature measured at the control building. Generally the lowest temperatures in the antenna are close to ambient, but occasionally they are less than ambient. This effect is partly due to radiative cooling to the sky and partly to the different location of the ambient temperature sensor.

There is a lot of structure evident on the temperature plots which may be compared with the external conditions of the antenna. In Fig. 3 the wind speed and antenna azimuth and elevation are shown along with the temperature plots. In this set of data there are clear indications that the temperature variations are related in some instances to the direction the antenna is pointing (marked with the bars) and at other times it is clearly correlated with the wind speed (arrows). The changes in antenna pointing correspond to moving the antenna between the source and a nearby astronomical calibrator. For most days of data examined it was not possible to definitely correlate the temperature changes with wind or antenna movements. Typically the wind time scales were similar to the interval between changes in antenna in the antenna pointing. The pointing change effect on temperature was usually clearest when there was a large direction change, such as a change of source.

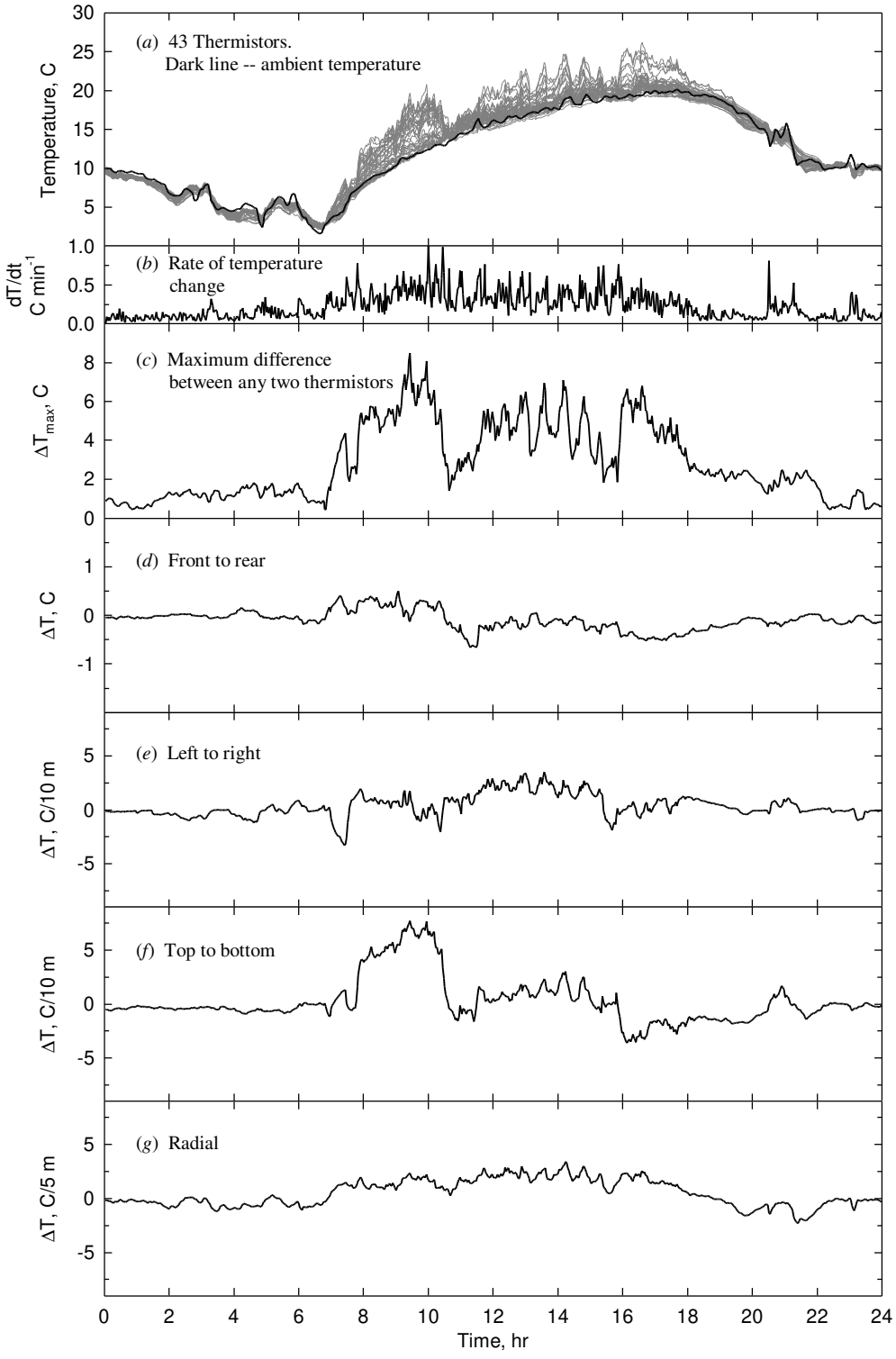

Figure 2: Data for 10 May 1998. (*a*) all temperature sensors. Solid line is ambient temperature, (*b*) maximum rate of change of temperature, (*c*) maximum difference, (*d*) average difference between front and rear sets of thermistors, (*e*) average gradient in azimuth direction, (*f*) average gradient in elevation direction, (*g*) average radial gradient.

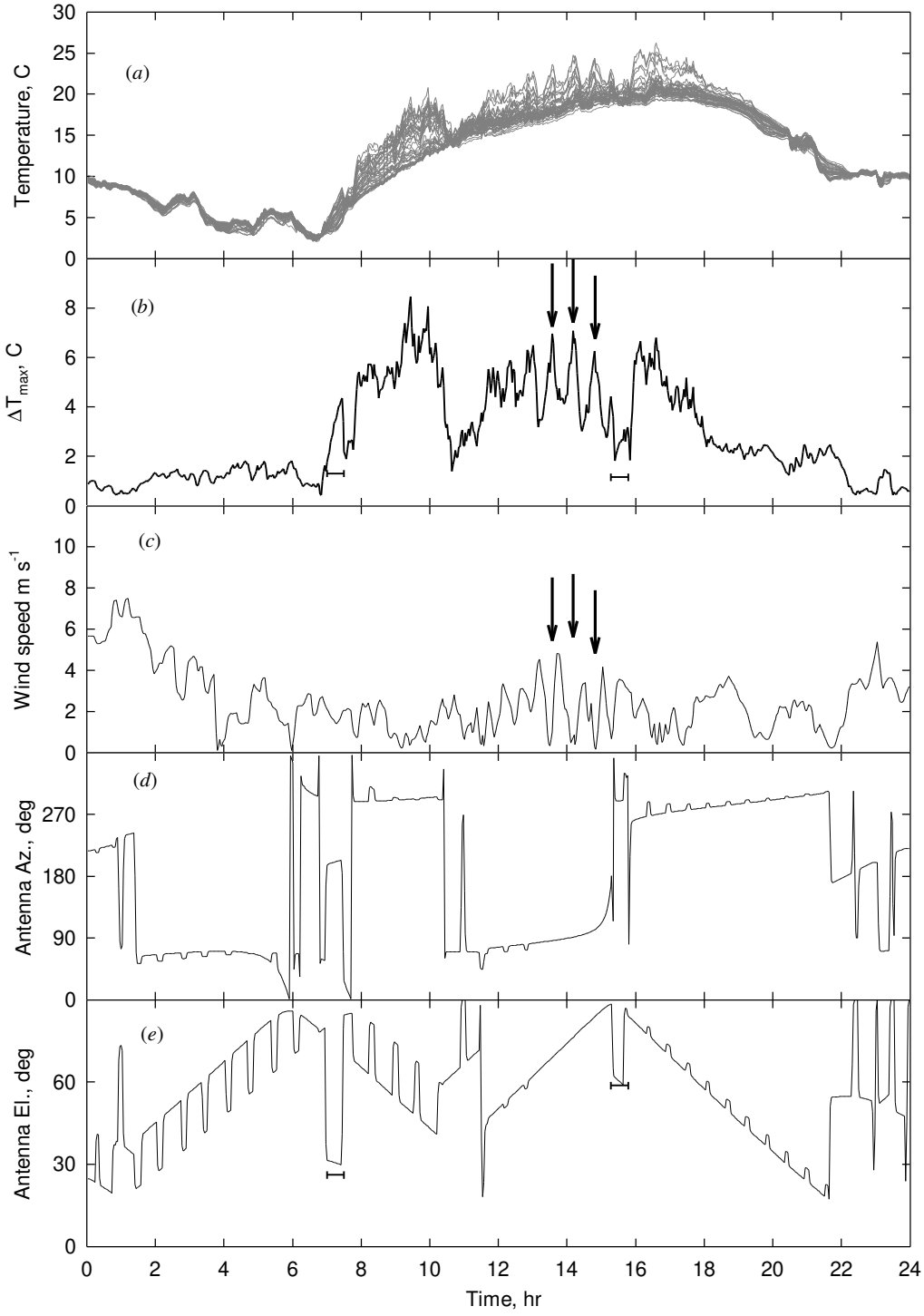

Figure 3: Correlation of temperature and environment. Structure in the temperature readings (*a*) and (*b*) is related to wind speed (*c*) indicated by the arrows, and to the antenna pointing direction (*d*) and (*e*) indicated by the bars.

To try to see these influences more definitely some statistical plots were made for 26 days of data (Figure 4). The graphs show the maximum ΔT versus the wind speed. Plots for daytime are separated according to whether the wind and the sun are from the forward or rear hemisphere of the antenna. All the data show that the wind reduces the maximum temperature gradient in the structure but, surprisingly, there is no obvious dependence on the sun or wind directions. Perhaps more correlation may be evident if the forward direction was defined as the solid angle where the BS is completely obscured by the dish surface, rather than taking the complete forward hemisphere. Some attempt has

been made to relate the measurements to the site for the MMA at 5 000 m elevation. The upper axis shows the wind speed at this site scaled to give the same heat transfer as corresponding speed at the OVRO site on the lower axis using the data from Cheng to account for the reduced air density [7].

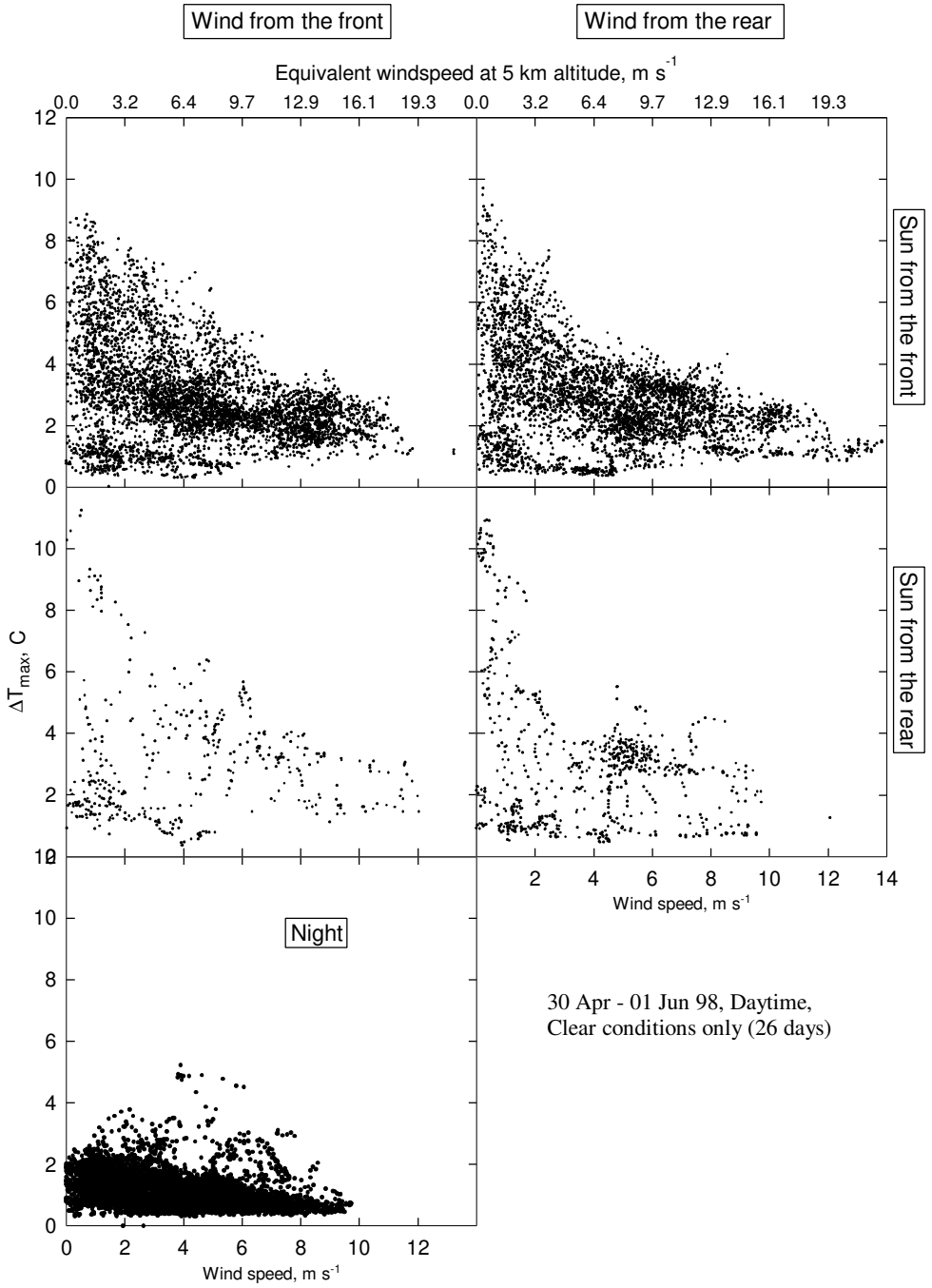

Figure 4: Dependence of maximum temperature gradient on wind speed. Daytime data are binned according to whether the sun or wind are in the front or rear hemisphere of the dish. The top axis shows the wind speed for equivalent cooling at a 5 000 m site.

One concern is whether taking just the maximum temperature difference between any two sensors is a good measure of the overall temperature variations. If, for example, one sensor is significantly different from the rest because of poor thermal contact, electrical problems, or extreme solar illumination it could skew the results. In this case the ratio of the rms to the maximum difference, $\Delta T_{rms}/\Delta T_{max}$ could be as low as 0.15 whereas for a uniform distribution the

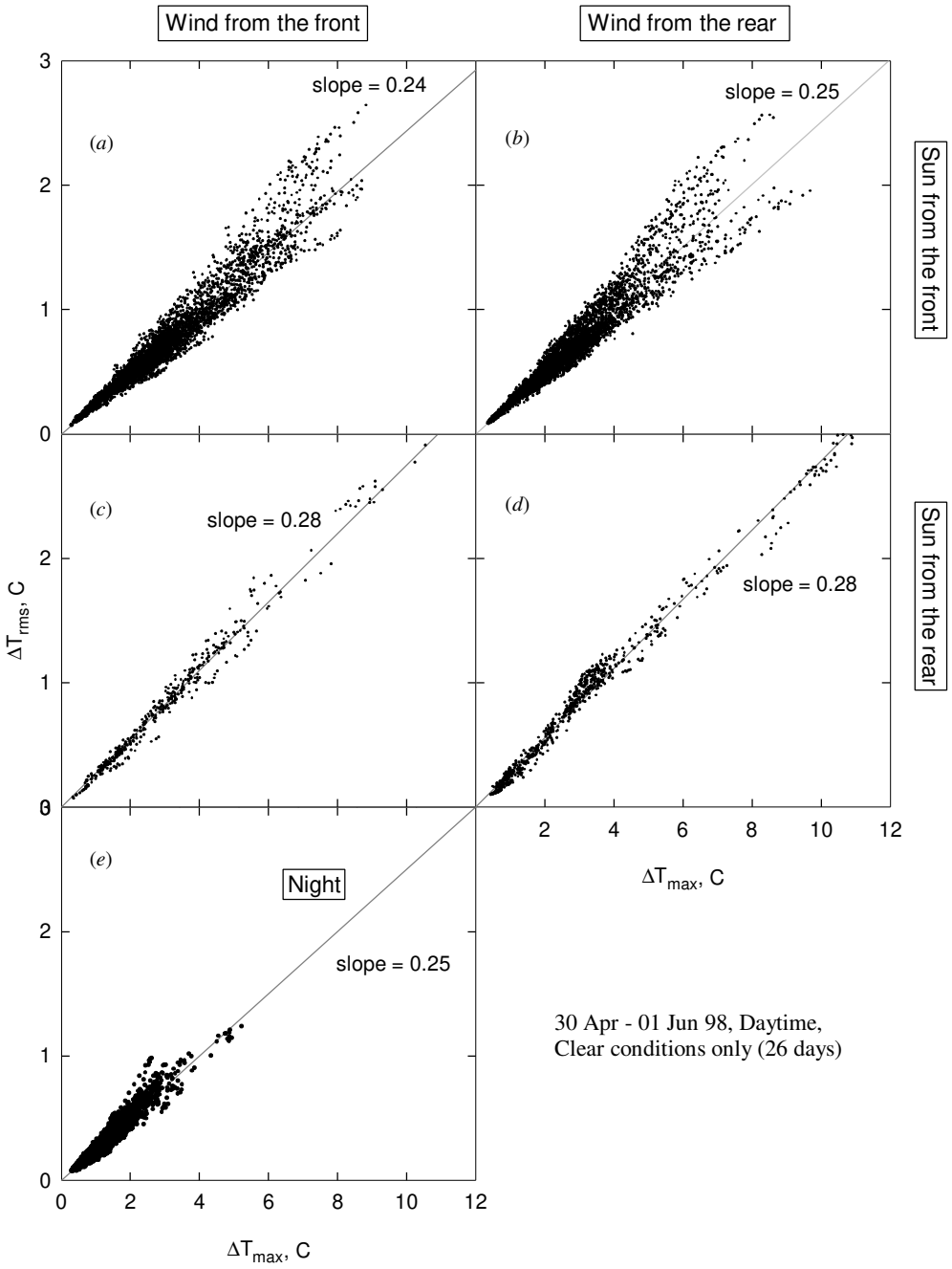

Figure 5: Relationship between the maximum temperature between any two sensors and the RMS of the whole set.

ratio should be 0.3 and for a normal distribution ~0.22. From the graphs in Fig. 5 the correlation between ΔT_{rms} and ΔT_{max} is very good and the values 0.24 – 0.28 is between the uniform and normal cases.

The distribution of $\Delta T_{\max}$ is given in Fig. 6. For the OVRO site the peak is around 0.7 C at night while the day time peak is 2.3 C. From the cumulative probability plot we see that for 95% of the time the maximum difference is below 5.6 C during the day and 1.8 C at night. This could be scaled to the MMA site using the wind distributions there compared to the Owens Valley.

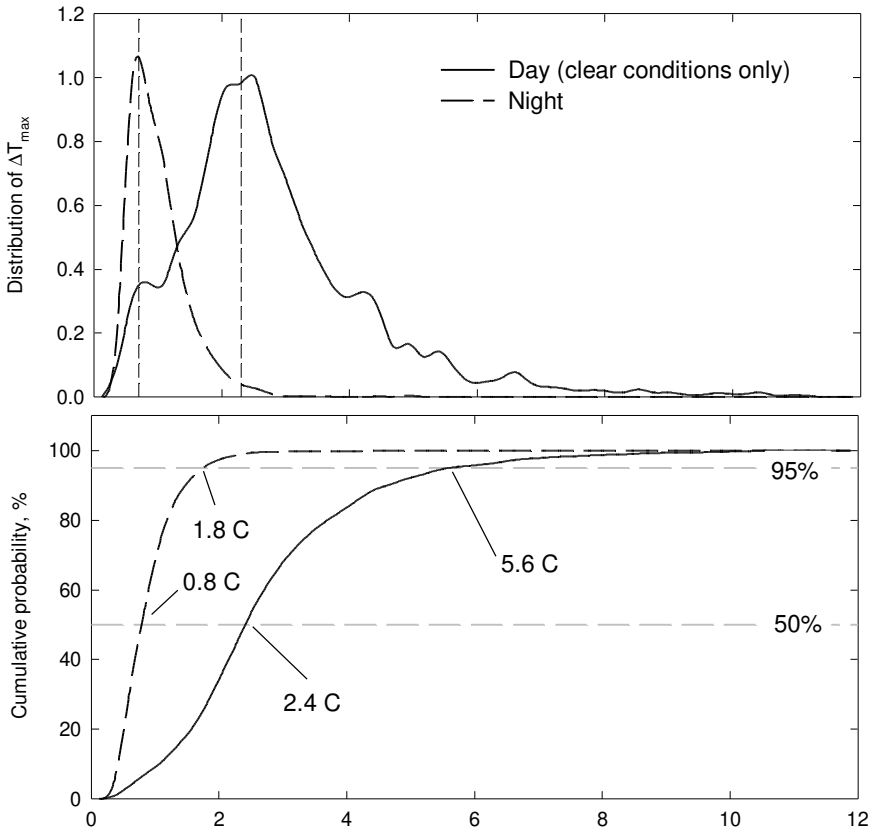

Figure 6: Distribution and cumulative probability for the maximum temperature difference.

4. Effect of Temperature on Backing Structure

The antenna BS is a triangular space frame comprising steel posts (parallel to the optical axis) and struts (approximately normal to the axis) with a total of five different cross-sectional areas (Fig. 7). A beam model (i.e., no rotational degrees of freedom at the nodes) was constructed using Algor [8], a finite element analysis program. The space frame is attached to a plate structure at nine points. In the model these were treated as constraints of the three translational degrees of freedom at each point, while the rotational degrees of freedom were left free. Clearly the details of the constraints influence the structural changes induced by applied temperature gradients. To minimize these effects the gradients applied were chosen so that these constrained nodes were close to the stress free temperature. To obtain the resulting pointing, focusing, and surface error terms a ray-tracing program was used to derive the parameters giving the minimum wavefront error. No aperture amplitude weighting was used, but this could easily be applied if required.

Some simple expressions relating pointing and focus to the temperature distribution were given in [2]. Equivalent temperature profiles were applied to the FEA model as a check. Uniform gradients were applied in the three orthogonal axes and radially to derive scale factors between temperature and pointing and focus. These are given in Table I. The original equation for the pointing error due to a lateral gradient in [2] was too small by a factor of two since the reflector tilt rather than the beam tilt was calculated. The analytical estimates are close enough to the numerical ones to be used as good working estimates for the order of magnitude of the effects. However the full FEA model is required to derive accurate numbers for a final antenna design.

Table 1: Comparison of analytical and numerical predictions of temperature gradients on pointing and focus of 10-m antennas.

	Pointing error [1] arcsec		Focus error mm		Residual Surface Error[3] µm
Gradient	**Analytical**	**Numerical[2]**	**Analytical**	**Numerical**	**Numerical**
1 C across width of reflector	0.19	0.28	0.000	0.000	0.5
1 C front to rear	0.00	0.00	0.510	0.404	3.8
1 C from center to edge	0.00	0.00	0.015	0.082	2.2

[1] This is without lateral refocusing to remove coma.
[2] Average over azimuth and elevation (see text).
[3] After focusing and pointing.

The influence of even relatively simple temperature profiles on the BS is complicated in detail. When a gradient in the vertical direction (dish at the horizon) is applied there is a pointing error which is not purely in the elevation direction but at about 9° to the vertical. This results from a slight asymmetry in the dish; there are diagonal members which cross the nominal symmetry plane from the rear on one side to the front on the other, all in the same sense. These are shown in the darker shading in Fig. 7. If all the struts had the same sectional area this would not cause the skew in pointing, but since the vertical posts and lateral struts are different, the asymmetry is reflected in the pointing. The situation is more complicated when the coma term is removed. To do this the secondary mirror needs to be moved a significant amount, partially canceling the pointing offset. The residual offset is reduced by a factor of four but and its direction now at 38° to the vertical. For a gradient in the horizontal direction the pointing shift is also in that direction but is slightly smaller than the vertical case.

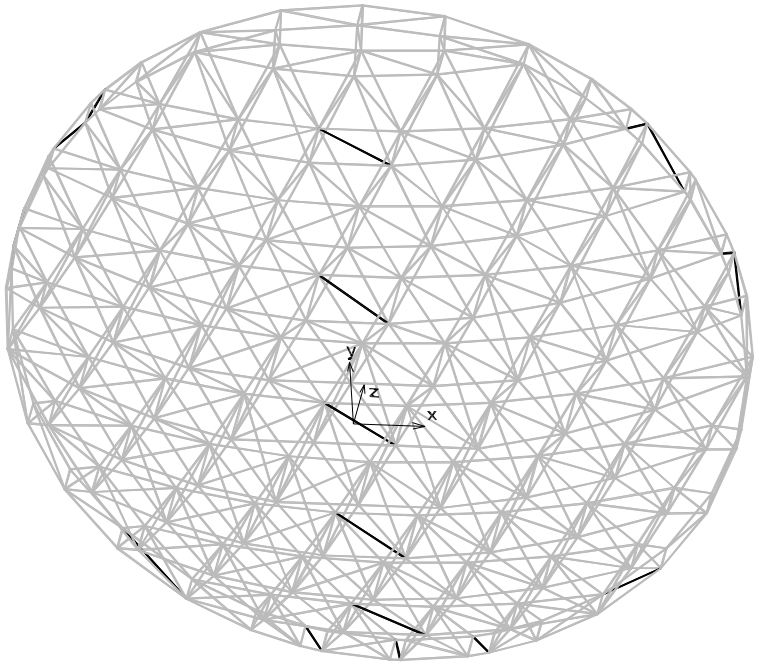

Figure 7: Model of the backing structure used in the FEA calculations. The dark struts are ones which break the lateral symmetry of the dish.

Real temperature data were also applied to the model. To interpolate between the thermistor positions an inverse distance weighting of all thesensors was used. Fig. 8 shows the results of applying the model to the data of Fig. 2. Fig. 8(*a*) shows the estimated effective surface error over a period of a day. Most of the error is in a linear gradient which can be removed by correcting the pointing offset, and refocusing removes much of the remainder. These two corrections reduce the peak error from ~50 µm to ~10 µm. The effect is even more pronounced when an error of 30 µm (representing panel errors, gravity, setting errors, etc.) is added in quadrature. Essentially all the thermal errors can be removed (Fig. 8(*b*)). Fig. 8(*c*) and (*d*) show the required corrections.

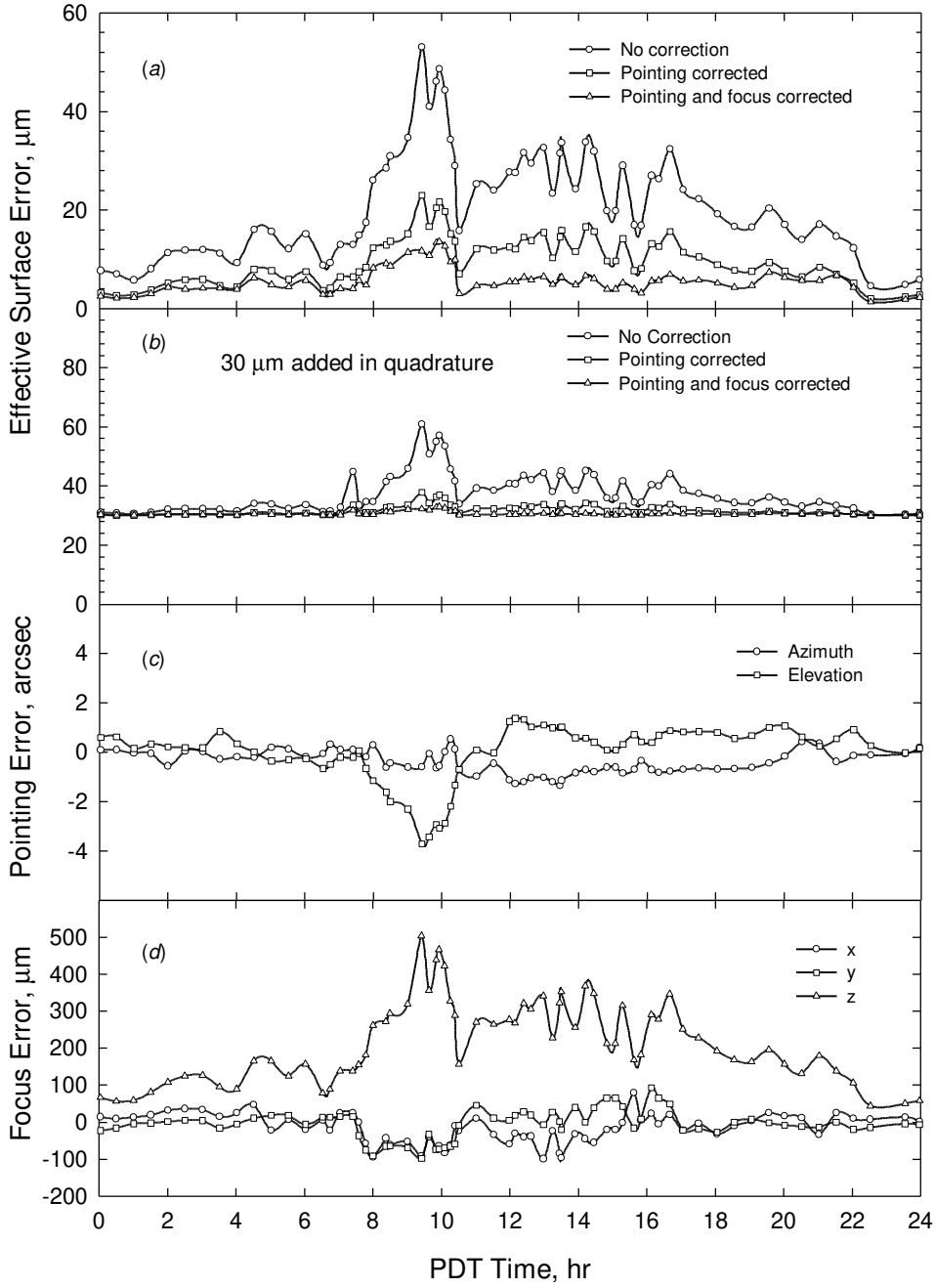

Figure 8: Surface error (*a*) and (*b*), pointing offsets (*c*), and focus error (*d*) derived from the FEA model using the data from Figure 2. In (*b*) 30 µm has been added in quadrature to represent other contributions to the surface error.

5. Discussion

Substantial temperature gradients are seen in the OVRO 10-m antennas during the day and these appear to affect mainly pointing and focus but have a relatively small effect on the actual surface error. Other antennas are known to show strong astigmatism under solar heating, but it is likely that this is comes from the mount and the way the backing structure is attached. We still have to investigate what the thermal behavior of the mount of the Leighton antennas is and how it couples into the backing structure shape, but current experience does not indicate any significant astigmatism. If this is so, inclusion of the temperature data into the telescope pointing and focusing algorithms would result in antenna performance which is virtually independent of the thermal environment.

Fig. 9 shows the pointing offsets which would be predicted by assuming that the offsets are proportional to the mean temperature gradients in the appropriate direction. The general shapes of the curves are similar to the full model results, but the differences are nevertheless significant. There is, in fact, no reason to assume that there should be a linear relationship between the temperature distribution and the structural deflections since the structural members are not homogeneous. Although a simple model would make the real time prediction easier, a complete solution of the model takes only a few seconds and is therefore viable as a part of an on-line correction scheme.

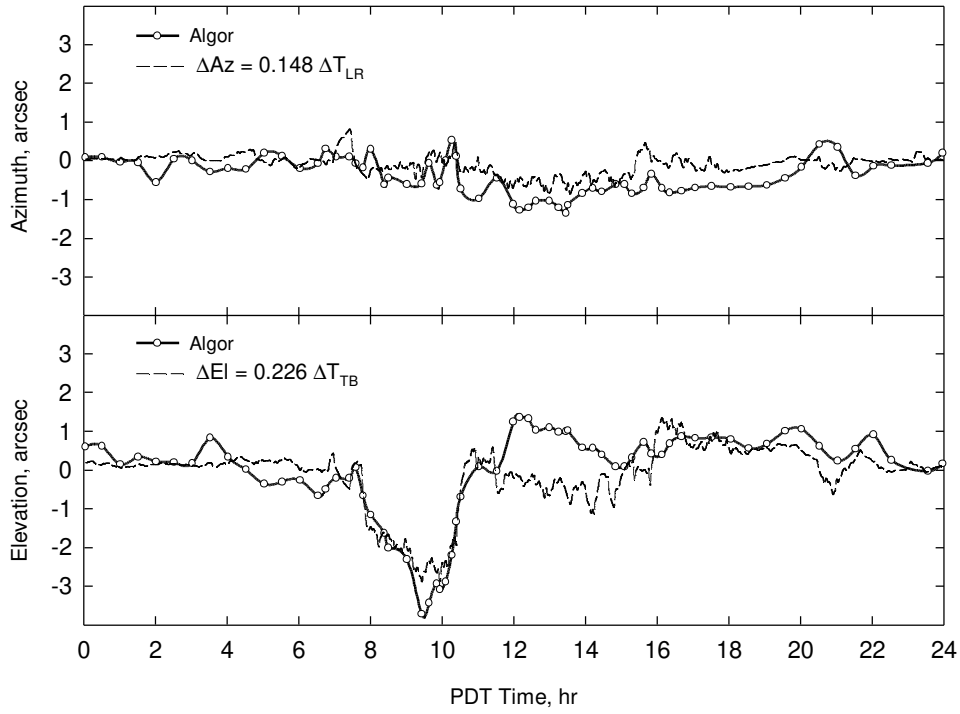

Figure 9: Comparison between the full FEA prediction for the pointing offset and an estimate based on a linear dependence on the temperature gradient.

As noted earlier, very rapid changes in temperature are seen in the data. Substantial changes occur within times of 10 min to 1 hr. This is consistent with the expected time constants for the materials under typical conditions of heat flow. Because of this, astronomical pointing and focus checks would have to be very frequent and the temperature monitoring scheme looks much more attractive. This is particularly true when it is considered that just the procedure of moving to a pointing source could change the temperature profile in the antenna.

What are the implications for the MMA? If an open type of backing structure is used these thermal measurements should be applicable with some small modification. The temperatures should not depend very much on the materials used but more on the surfaces. If carbon fiber reinforced plastic (CFRP) is used it would also be finished with a high reflectance white paint. The time constants for the changes may be faster for the CFRP: although it has a higher specific heat, a strut would have less mass than a steel member of equivalent stiffness. However, since the expansion would be dominated by the steel nodes, these would control the time constants also.

The effects of the reduced air density have been discussed earlier. Ideally the design should not rely significantly on cooling by the wind since there will be times, particularly in the morning, when the wind is low but solar heating is strong. Slightly higher temperatures than the no-wind ones measured at OVRO may be expected since the T^4 dependence of radiative cooling effectively counteracts the reduction in convective and conductive cooling. Since the site is higher and further south than OVRO the solar flux will be higher, which will also increase the temperature gradients somewhat. It seems reasonable to assume that a gradient of 10 C across the BS would cover most conditions.

CFRP is still a reasonable choice for the MMA since the requirements on surface accuracy and pointing are more stringent than for the OVRO and the thermal climate of the site harsher. With careful design a combination of CFRP struts and steel nodes should approach a factor of ten improvement over an all-steel construction. With the active use of temperature measurements we would not expect to do better than a factor of five. If it proved desirable it would be straightforward to retrofit antennas with thermistors as an additional layer of thermal control.

Further work is in progress to instrument the mount and secondary mirror supports of the OVRO antenna. We also propose to experimentally check the correlation between the temperatures and pointing, and possibly focus. Since the measurements reported here the thermistor blocks have been painted with the same paint as the BS to ensure that there are no important differences between the thermistors and the steel. If such differences exist in the data they probably err on the pessimistic side so the conclusions drawn here should not be invalidated.

6. References

[1] R.B. Leighton, Final Technical Report for National Science Foundation Project AST 73-04708
[2] J.W. Lamb: "Thermal considerations for mmA antennas," NRAO MMA Memo #83, May 1992.
[3] YSI Incorporated, Yellow Springs, Ohio 45387, USA.
[4] J.W. Lamb and R. Forster: "Temperature Measurements on BIMA 6-m Antennas—Part I: Backing Structure," NRAO MMA Memo #100, Oct. 1993.
[5] National Instruments Corporation, 11500 N Mopac Expwy, Austin, TX 78759-3504.
[6] Emerson and Cuming Microwave Products, Canton, Randolph, USA.
[7] J. Cheng: "Forced air cooling at high altitude," NRAO MMA Memo #203, March 1998.
[8] Algor, Inc. 150 Beta Drive, Pittsburgh, PA 15238-2932, USA.